Experimental Analysis of Air-Water Heat Exchanger with Microchannel Coil Exposed to Different Working Parameters

Vladimir Glazar, Anica Trp, Kristian Lenic, Mateo Kirincic

University of Rijeka, Faculty of Engineering, Department of Thermodynamics and Energy Engineering, Vukovarska 58, Rijeka, HR-51000, Croatia

Abstract

In this study experimental analysis of heat exchanger with microchannel coil (MCHX) has been done. MCHX have already been proven as key for improvement of outdoor condenser units in domestic space cooling systems. Many questions still exist in case of their implementation as evaporating unit, or in case of both single and multi-phase fluid flow. In this study MCHX is used as air-water heat exchanger. An open circuit wind tunnel has been used for testing the MCHX in this non-standard application. The experimental analysis has been performed for a range of various water/air velocities and temperatures. Water temperatures and velocities, as well as air temperatures, velocities and pressure drops, were measured using data acquisition system with developed application in *Labview* software. Influence of water/air inlet temperatures and velocities on heat transfer in the heat exchanger with microchannel coil has been investigated.

Keywords: Microchannel heat exchanger, open circuit wind tunnel, experimental analysis

1. Introduction

Development of heat exchangers and search for higher heat transfer rate per volume brought new group of compact heat exchangers: the heat exchangers with microchannel coil (Kandlikar et al., 2016). The heat exchanger with microchannel coil (further in text: MCHX) consists of flat tubes and folded fins that are connected to the manifolds. In last decades, mostly used as automotive radiators and condensers, they have a great potential in a field of domestic space heating and cooling systems. MCHX have already been applied as a standard part of air conditioning units, refrigeration systems, transport cooling systems, and even as high efficient chilled water coils for air conditioning and process cooling (Danfoss, 2018). Better performance, lower weight compared to standard copper fin-and-tube heat exchangers, minimal use of refrigerant and easier handling are just some of advantages and reasons for their larger implementation. Consequently, increased savings can be obtained by use of MCHX as a unit in single phase heat exchange, or in processes where phase change occurs. However, all aluminium MCHX still lack broader appliance in case when they should be applied as evaporators where refrigerant mal-distribution should be taken with special caution. Liquid/gas separation, control of the refrigerant flow direction, secondary openings to spread out the refrigerant evenly across the length of the manifold, are just some of designs developed to make possible this use of MCHX (Kaltra Inovativtechnik, 2018).

Large number of research papers about MCHX can be found with different topics that deal with both single phase or with phase change processes (Asadi et al., 2014). Al-Zaidi et al. (2018) made experimental investigation to study the effect of refrigerant flow rate, local vapour quality, coolant flow rate and its inlet temperature on the local condensation heat transfer coefficient. They compared their experimental results with the existing correlations for the heat transfer rate. Dalkilic et al. (2017) published results of their experimental study of heat transfer characteristics of single-phase flow. In paper, they investigated single-phase turbulent flow of R-134a refrigerant in a rectangular multi-micro channel heat sink. Their finding demonstrated that well-known correlations for heat transfer could be used to predict heat transfer in multiport microchannel heat sink. This is very important, as in last decade of twentieth century respectable number of papers with experimental data for friction factor and Nusselt number in microchannel disagreed with conventional theories. Morini (2004, 2006), and later Rosa (2009), concluded that when dealing with microchannels, standard theory and correlations can be used but with inclusion of scaling effects that are often neglected. Dalkilic et al. (2018) investigated flow boiling

doi:10.18086/eurosun2018.01.04 Available at http://proceedings.ises.org

of refrigerant R134a inside a multi-microchannel heat sink. They developed the copper test section that consisted of 27 parallel rectangular channels with all dimensions smaller than 0.5 mm. Using data collected by the experiments they proposed new correlation to calculate the heat transfer coefficients for R134a flow boiling inside the multi-microchannel at high mass flow and high heat fluxes. Application in single phase process has been given by Robles et al. (2014). In paper, authors examined aluminium minichannel solar water heater performance under year-round weather conditions. In case of solar water heaters, increase of the heat transfer efficiency can be obtained using a more compact design of heat exchangers with microchannel technology (Garcia et al., 2011). Bhuiyan and Sadrul Islam (2016) have done review of research papers about heat exchangers geometry. They explored thermal and hydraulic performance of finned-tube heat exchangers under different flow regimes. Knourek et al. (2012) showed by detail set up and procedures that they used for measurement of thermal characteristics of the heat exchangers in their laboratory. They showed measured results for common automotive water-air heat exchanger by mean of normalized heat exchanged at the coolant side and by normalized heat exchanged at the air side.

In this paper, experimental analysis of the water-air heat exchanger with microchannel coil, that has been installed and tested in wind tunnel in its non-standard application, has been presented. Single-phase heat transfer characteristics have been measured and analysed. Thus, the influence of water/air inlet temperatures and influence of different velocities on heat transfer has been investigated. For purpose of this experimental investigation, previously developed open circuit wind tunnel (Glazar et al., 2011; Glazar et al., 2015) has been modified and upgraded. Description of experimental facility setup, test conditions and methods, with measurement results and final conclusions follows.

2. Experimental Facility

2.1. Open circuit wind tunnel

The experimental measurements have been done in open circuit wind tunnel, shown on Figure 1, which is used to prepare air and bring it towards measuring zone.

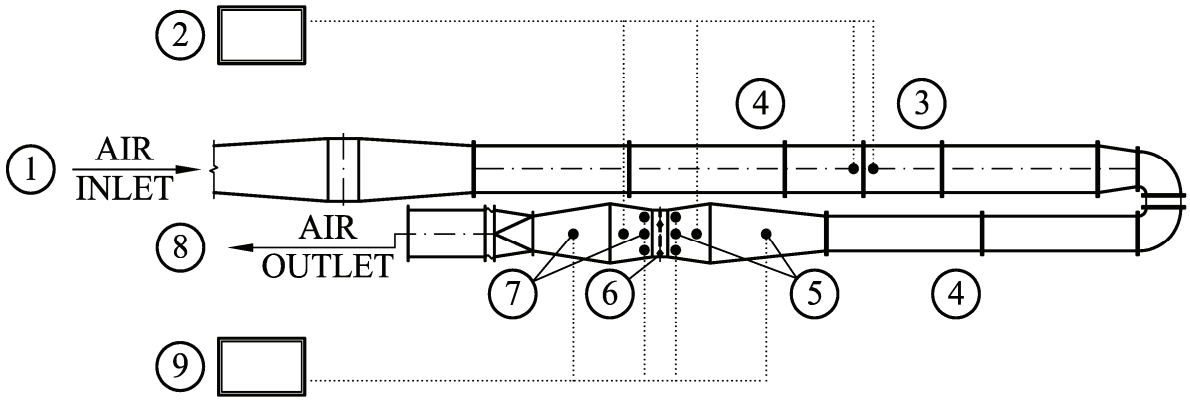

LEGEND: 1. air inlet (from air handling unit), 2. data acquisition system for pressure drops, 3. orifice, 4. air settling ducts, 5. air inlet temperature and air inlet velocity sensors, 6. MCHX (with installed water temperature in/out sensors), 7. air outlet temperature and velocity sensors, 8. air outlet, 9. data acquisition system for velocities and temperatures

Fig. 1: Schematic view of experimental facility (wind tunnel)

The main components of the system are air supply unit with centrifugal fan, measuring orifice, heat exchanger with microchannel coil, instrumentations and data acquisition systems. The open circuit wind tunnel system, containing air-handling unit with heating and cooling section, is used to draw air over the tested heat exchanger. The air flow rate can be adjusted by pressure relief damper from approximately 20 to 100% of maximal air flow rate. The upper part of tunnel is composed of circular ducts with diameter of 600 mm and the lower part consists of rectangular ducts of appropriate size, 550 x 450 mm.

2.2. Water-based heating/cooling loop

The hot/cold water supply section is divided in two separate loops. Primary loop with hot/cold water is connected to water/water heat pump with capacity of 50 kW and to the building heating installation. Secondary water loop is connected to the primary water loop with plate heat exchanger as shown on Figure 2. Secondary loop is used to prevent possible creation of lime scale in micro channels and it is filled with demineralized water. Lime scale is extremely damaging for channels with hydraulic diameter smaller than 1 mm and could cause undesired obstructions on water side of heat exchanger if not carefully treated.

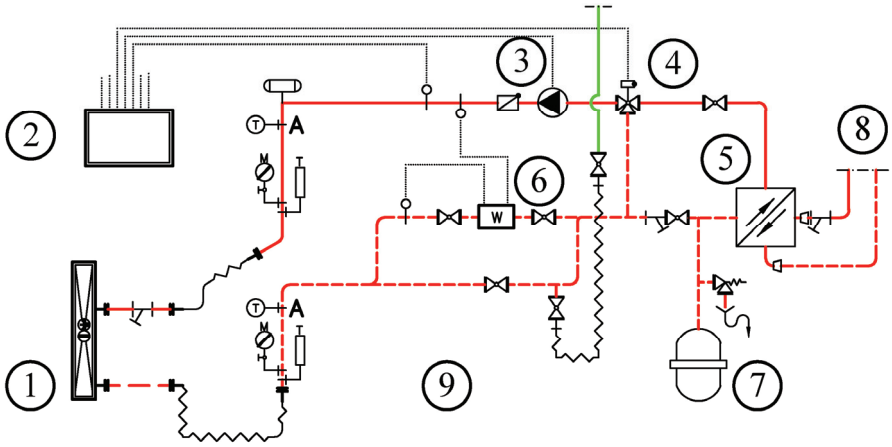

LEGEND: 1. test heat exchanger (MCHX), 2. hot/cold water control unit, 3. water pump, 4. three-way regulating valve, 5. plate heat exchanger between primary and secondary water loops, 6. ultrasonic flow meter, 7. expansion vessel, 8. connection to primary water loop, 9. secondary water loop filled with demineralized water

Fig. 2: Schematic view of water loop filled with demineralized water

2.3. Temperature and flow measurements

The air inlet and air outlet temperatures were measured with two thermocouple fields each placed before and after MCHX. Thermocouple field placed before MCHX was composed of three *K* type thermocouples. Thermocouple field placed after MCHX was composed of twelve *K* type thermocouples. Water inlet and outlet temperatures were measured with two thermocouples. Used thermocouples were pre-calibrated with an accuracy of ±0.15°C. Signals obtained from all temperature sensors were recorded and then processed. Figure 3a shows measuring station of wind tunnel with installed data acquisition system and part of secondary water loop with pipes filled with demineralized water. Figure 3b shows thermocouples' displacement.

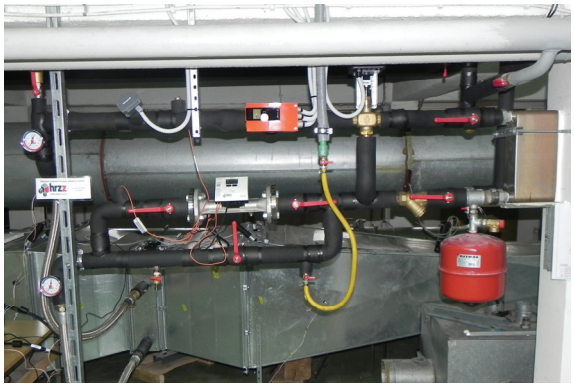

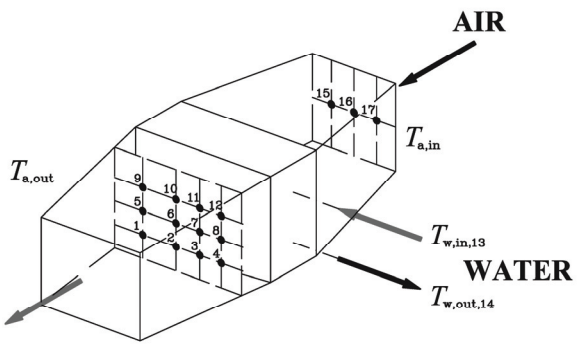

(a) **(b)**

Fig. 3: Measuring station of wind tunnel (a) and layout of thermocouples' fields (b)

Measuring orifice was used to determine air volume flow rate in orifice opening. Air passing through an orifice construction creates pressure drop in system. Pressure drop was measured with portable measuring system. Following equation has been used to calculate volume flow rates for each measurement setup:

$$\dot{V}_a = \alpha \cdot \varepsilon \cdot A \cdot \sqrt{\frac{2 \cdot \Delta p}{\rho_a}} \qquad \text{(eq. 1)}$$

where used variables represent:

$\dot{V}_a$ - air volume flow rate, $m^3\ s^{-1}$,

α - pipe orifice flow coefficient, -,

ε - coefficient of discharge, -,

A - cross-sectional area of the orifice hole, m^2,

ρ_a - air density, $kg\ m^{-3}$ and

Δp - measured pipe orifice pressure drop, Pa.

Corresponding average air velocity in ducts and air mass flow rate have then been calculated according to acquired air volume flow rate. Additionally, four hotwire anemometer probes (Figure 4a) were used to measure air velocities at appropriate cross-section of the tunnel. These data have been used to validate previously calculated air mass and volume flow rates. Time-wise air velocities, measured for three measuring points, have been shown on figure 4b.

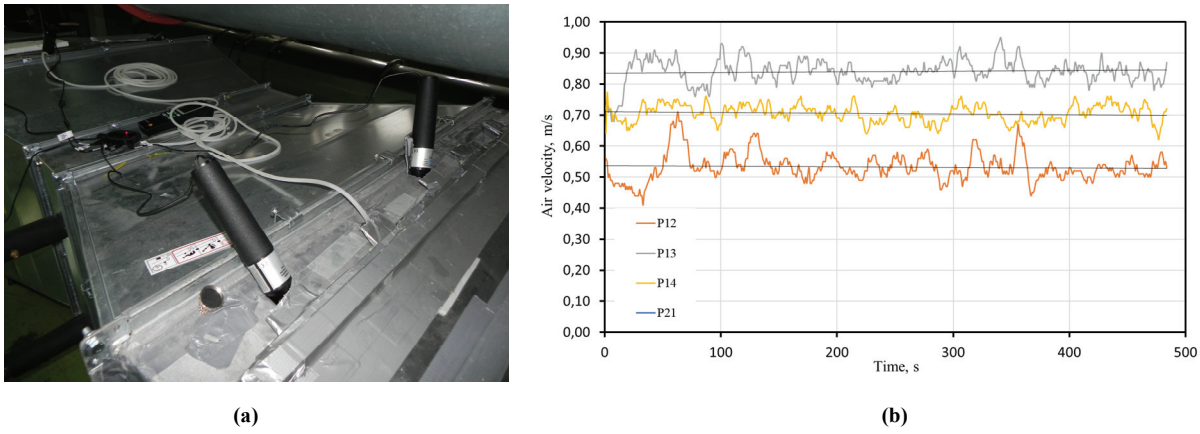

(a) **(b)**

Fig. 4: Set up of hotwire anemometer probes (a) and graph-chart with measured air velocities at three points (b)

Water volume flow rate inside secondary water loop was measured with ultrasonic water flow meter. Appropriate water velocities and water mass flow rates were calculated according to previously measured water volume flow rates. Required water flows were obtained by change of water pump rotor speed.

2.4. Data acquisition system

The National Instruments SCXI data acquisition, automation and control module system was used. Connection to personal computer has been done by National Instruments USB-6251 adapter. All virtual instruments were developed in *LabVIEW*. Figure 5a shows data acquisition system connected to personal computer and Figure 5b shows user interface developed for purpose of these measurements.

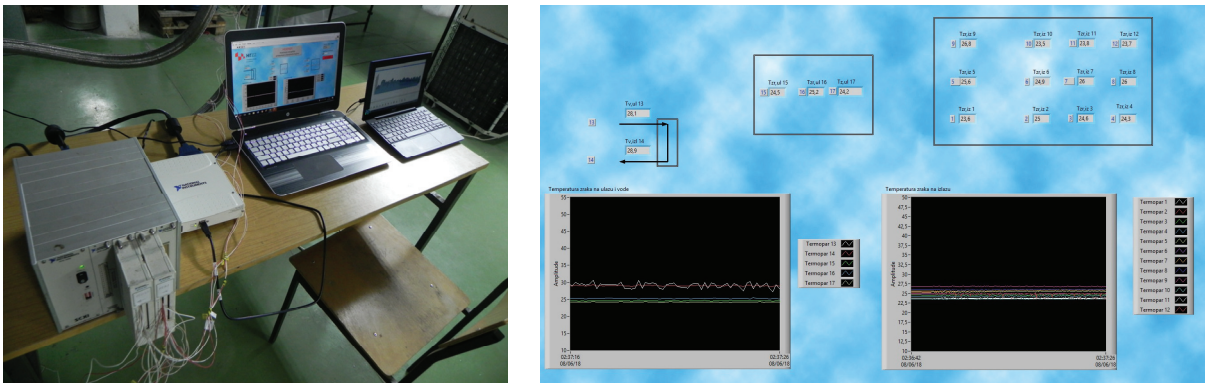

(a) (b)

Fig. 5: Data acquisition system (a) and graphical user interface (b)

Experimental data are automatically saved to data file for further analyses. Block diagram section of developed virtual instrument in *LabView* is shown on Figure 6.

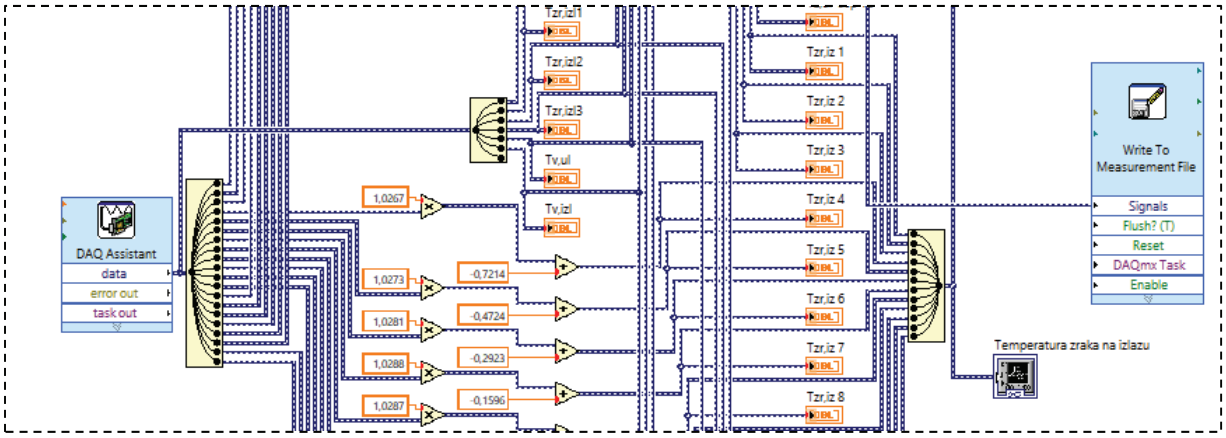

Fig. 6: Section of virtual instrument's block diagram developed in *LabView*

2.5. Test heat exchanger

The MCHX used in this investigation consist of 47 parallel flat tubes connected with louvered fins. Flat extruded tubes contains multiple small rectangular channels, each with hydraulic diameter smaller than 1 mm. Outer overall dimensions of tested heat exchanger are 860 x 600 mm. MCHX has two passes. The first pass includes approximately 3/4 of all tubes and the second pass is made of remaining tubes. Figure 7a shows heat exchanger before it was installed in measuring station and figure 7b shows thermogram of MCHX surface temperatures distribution during steady state condition.

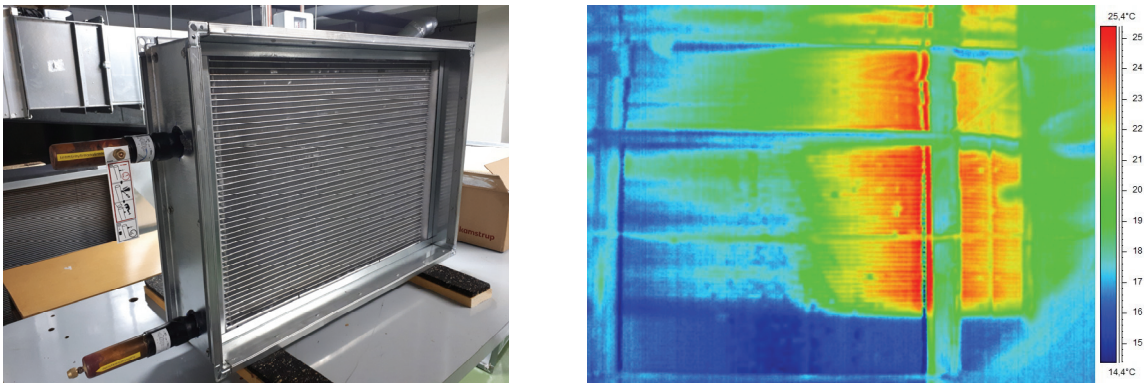

(a) (b)

Fig. 7: MCHX (a) and thermogram of MCHX surface (b)

Thermogram of MCHX surface, made by infrared camera during experiment, gives clear insight in water flow through heat exchanger tubes. Division of water flow from first to second passage can be well noticed through MCHX surface temperature distribution because of extensive water-cooling. In this work, thermograms were used for qualitative assessment of heat exchanger's surface temperature distributions.

3. Measurement conditions and results

3.1 Test conditions

Measurements were performed for a wide range of air and water velocities and temperatures. Air inlet velocities were in a range from 0.5 to 5 m s^{-1}. Water velocities entering in heat exchanger were in a range from 0.05 to 1 m s^{-1}. Both air and water temperatures were in range from 2 to 67°C. A series of experimental measurements have been done in order to analyse heat transfer in the heat exchanger with microchannel coil. Set of different parameter setups have been created according to measurement plan. Two major groups of measurement setups have been performed: first with air inlet temperatures in the range from 10 to 15°C, and second with air inlet temperatures in the range from 20 to 25°C. Time wise air and water temperatures for test conditions: $T_{w,in}$ = 50°C, $T_{a,in}$ = 20°C, $u_{w,in}$ = 0.1 m s^{-1} and $u_{a,in}$ = 0.7 m s^{-1}, are shown on Figure 8a (startup procedure) and Figure 8b (steady state). Data acquisition frequency in all measurements was set to 1 Hz.

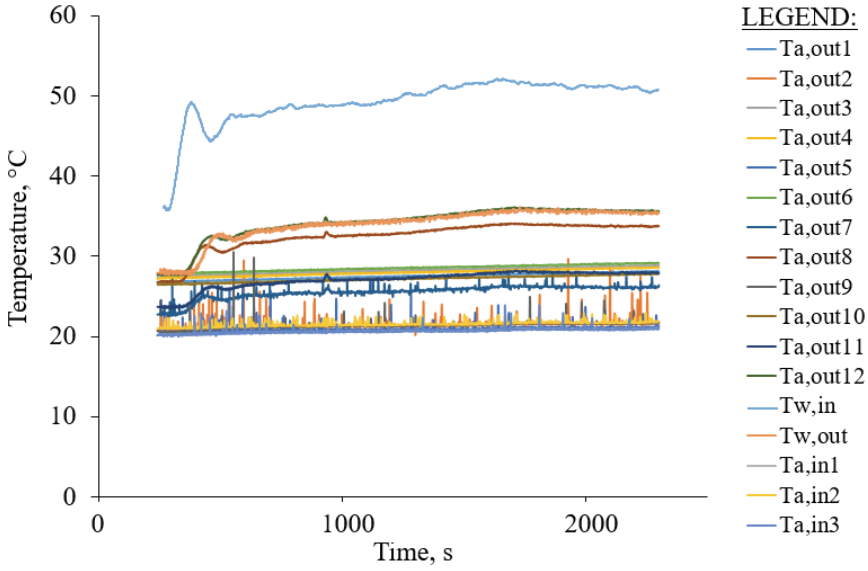

(a)

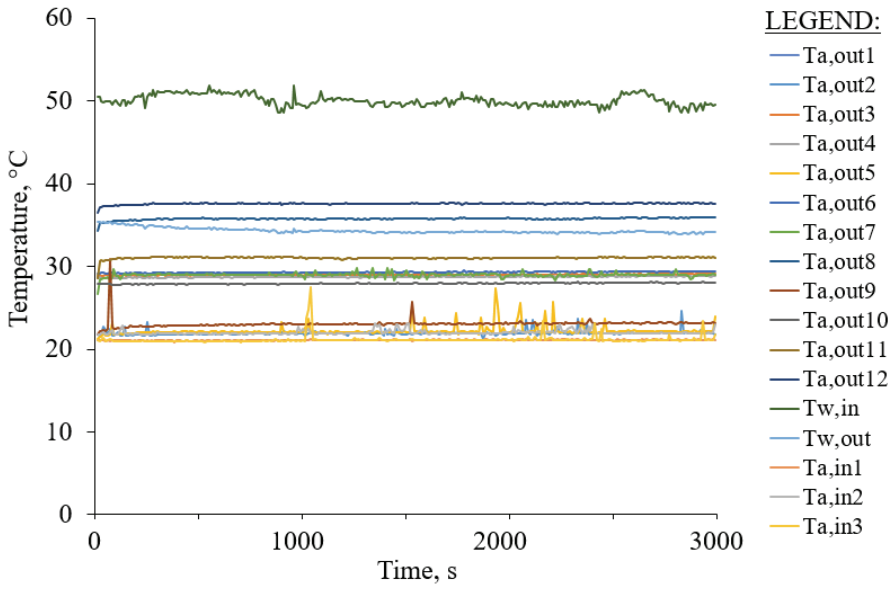

(b)

Fig. 8: Air and water temperatures for heating startup procedure (a) and after steady state achieved (b)

All measuring data were collected for steady-state conditions. Error analysis has been done according to standard procedures. As a part of the analysis, the balance of measured exchanged heat fluxes on water and air side has been checked.

3.2 Average temperatures and exchanged heat fluxes

Measurement results have been given by corresponding exchanged heat fluxes. Heat fluxes were calculated using average air and water temperatures as well as air and water velocities acquired by experimental measurements. Average temperatures of air were calculated from multiple temperature measuring points using following equations:

$$T_{\mathrm{a,in}} = \frac{\sum_{i=1}^{3} T_{\mathrm{a,in\ i}}}{3} \qquad \text{(eq. 2)}$$

$$T_{\mathrm{a,out}} = \frac{\sum_{i=1}^{12} T_{\mathrm{a,out\ i}}}{12} \qquad \text{(eq. 3)}$$

Average exchanged heat flux can be expressed as:

$$\dot{Q}_{\mathrm{m}} = \frac{\dot{Q}_{\mathrm{w}} + \dot{Q}_{\mathrm{a}}}{2} \qquad \text{(eq. 4)}$$

where air side and water side heat fluxes can be calculated by:

$$\dot{Q}_{\mathrm{w}} = \dot{m}_{\mathrm{w}} \cdot c_{\mathrm{w}} \cdot \Delta T_{\mathrm{w}} \qquad \text{(eq. 5)}$$

$$\dot{Q}_a = \dot{m}_a \cdot c_{P,a} \cdot \Delta T_a = \rho_a \cdot \dot{V}_a \cdot c_{P,a} \cdot \Delta T_a \qquad \text{(eq. 6)}$$

In previous equations used variables are:

$c_{P,a}$ - specific heat capacity of air, J kg^{-1} K^{-1},

c_w - specific heat capacity of water, J kg^{-1} K^{-1},

$\dot{m}_a$ - mass flow rate of air, kg s^{-1},

$\dot{m}_w$ - mass flow rate of water, kg s^{-1},

ρ_a - air density, kg m^{-3},

$\dot{Q}_a$ - air side heat flux, W,

$\dot{Q}_m$ - average exchanged heat flux, W,

$\dot{Q}_w$ - water side heat flux, W,

ΔT_a - air temperature difference, K,

ΔT_w - water temperature difference, K,

$T_{a,in}$ - air inlet temperature, K and

$T_{a,out}$ - air outlet temperature, K.

3.3 Measurement results

Results are given for heat exchanger with microchannel coil in single-phase heat transfer conditions. Calculated heat fluxes on air and water side, combined with average exchanged heat flux for range of different water velocities are shown on Figure 9. Test conditions for this measurements were: $T_{w,in}$ = 35°C, $T_{a,in}$ = 24°C and $u_{a,in}$ = 0.7 m s^{-1}

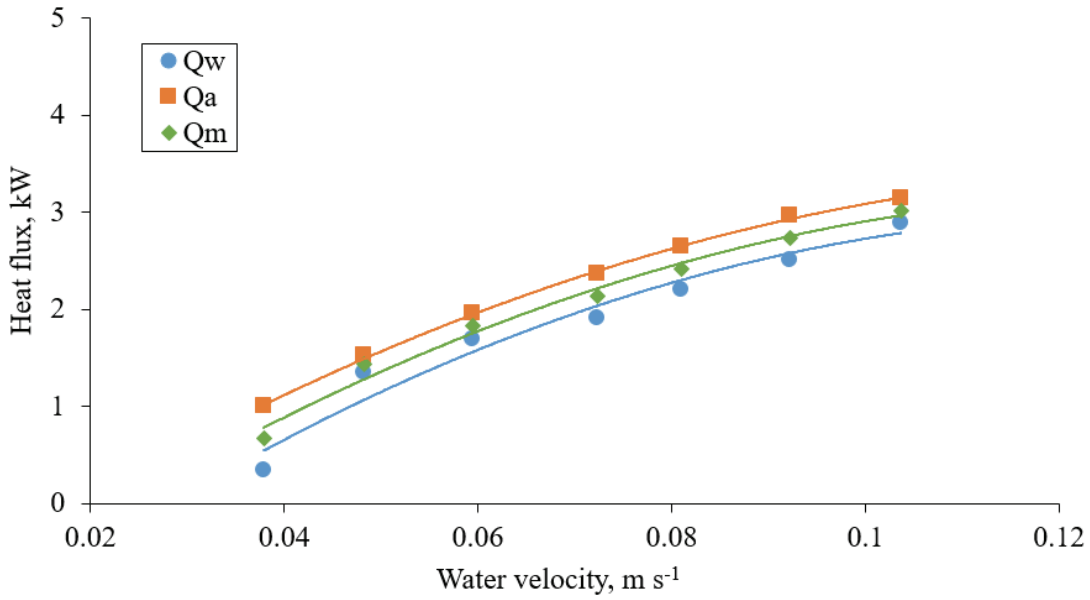

Fig. 9: Exchanged heat fluxes on air and water side combined with average exchanged heat flux for different water velocities. Test conditions: $T_{w,in}$ = 35°C, $T_{a,in}$ = 24°C and $u_{a,in}$ = 0.7 m s^{-1}

Average air inlet and air outlet temperatures were used to calculate heat fluxes on air side and measured water inlet and outlet temperatures were used to calculate heat fluxes on water side. Heat fluxes, both on air and water side, were higher at higher water inlet velocities. In this measurement setup, calculated air heat fluxes were higher than water heat fluxes for all water velocities as can be seen from Figure 9.

Air outlet temperatures and average exchanged heat fluxes for the range of water inlet velocities from 0.03 to 0.12 m s^{-1} are shown on Figures 10a and 10b. Corresponding water flow rates were from 150 to 480 l h^{-1}. Air inlet temperature was 22°C, air inlet velocity was 1.58 m s^{-1} and water inlet temperatures were 35, 40, 45 and 50°C.

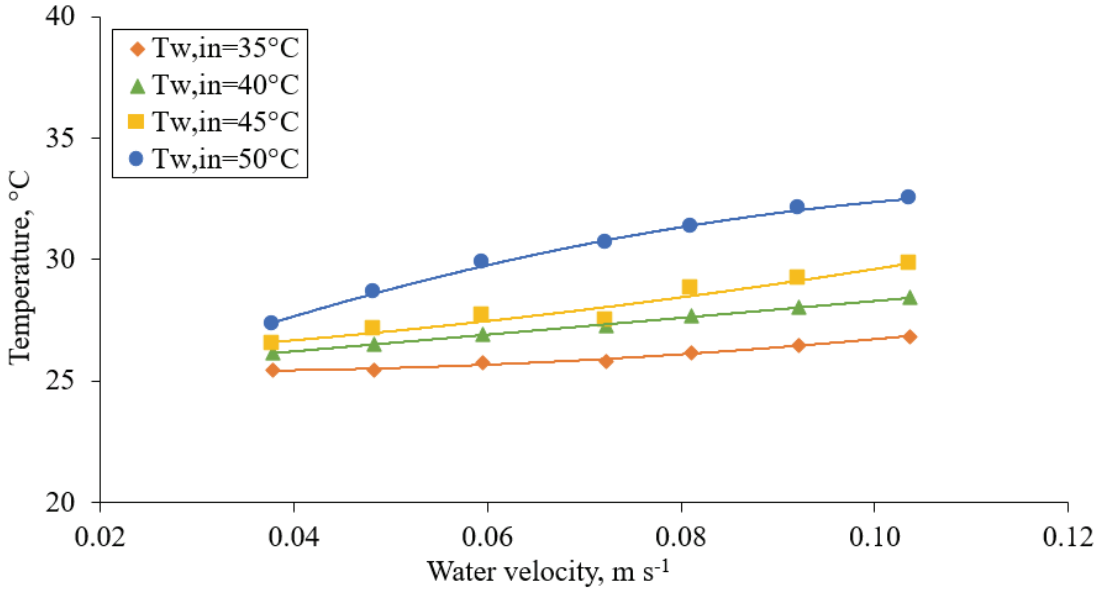

(a)

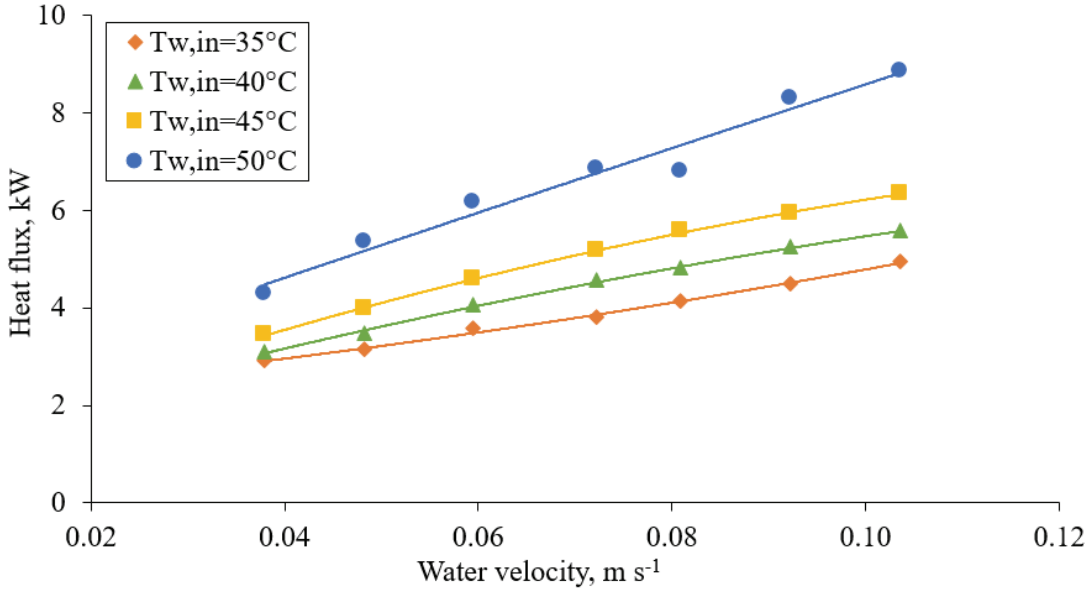

(b)

Fig. 10: Air outlet temperatures (a) and average exchanged heat fluxes (b) for different water velocities and water inlet temperatures. Test conditions: $T_{a,in}$ = 22°C, $u_{a,in}$ = 1.58 m s^{-1}

Higher water velocity gives higher heat flux for constant water inlet temperature. In case of lower water velocities, the differences between heat fluxes for different water temperatures are relatively small and they increase with higher water velocities.

Figure 11 gives insight in temperature and heat flux changes depending on water velocity for two different air inlet velocities. In this measurements air inlet temperature was 22°C and water inlet temperature was 40°C.

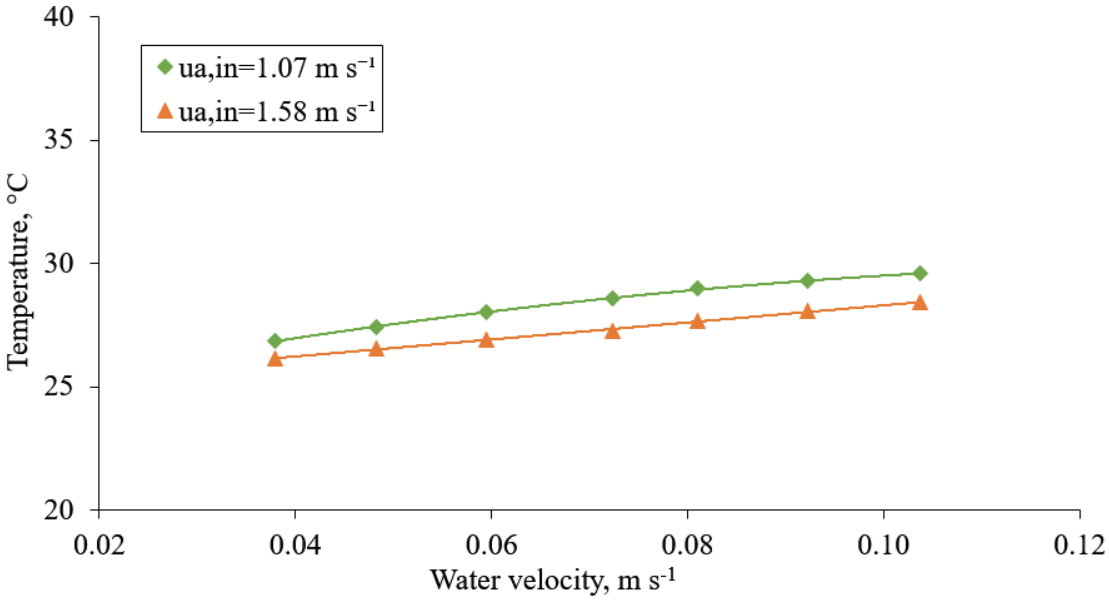

(a)

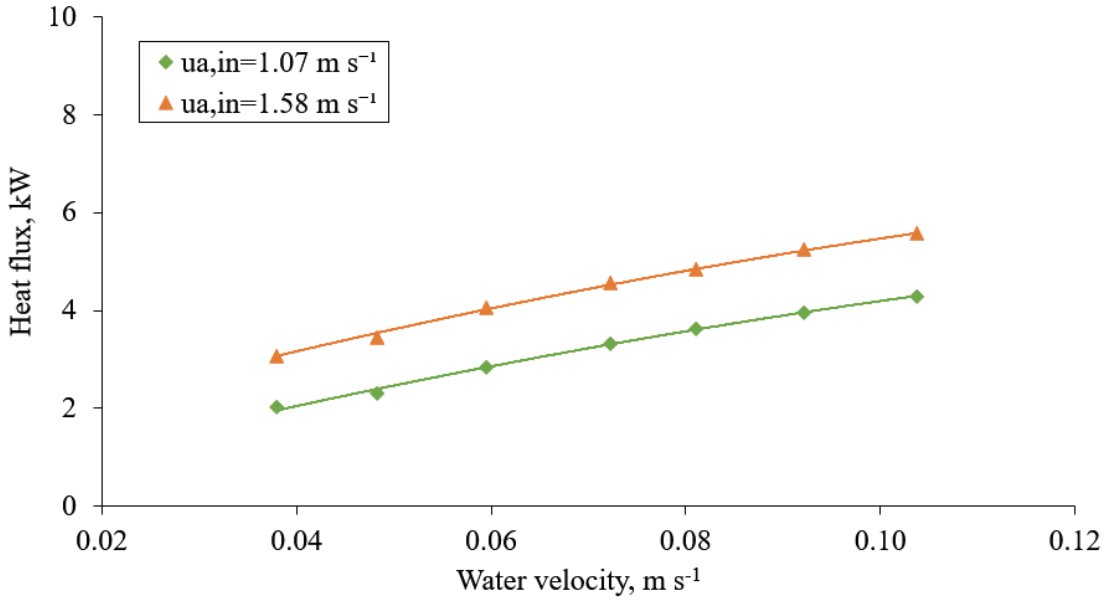

(b)

Fig. 11: Air outlet temperatures (a) and average exchanged heat fluxes (b) for different water and air velocities and inlet temperatures. Test conditions: $T_{a,in}$ = 22°C, $T_{w,in}$ = 40°C

Measured air outlet temperatures are lower in cases of higher air velocities. Heat fluxes have higher values with increasing of air and water velocities.

Heat fluxes for measured range of water inlet temperatures are shown for two different water inlet velocities (Figure 12a) and for two different air inlet velocities (Figure 12b). Air inlet temperature was 12°C, air inlet velocities were 1.16 m s^{-1} and 1.43 m s^{-1}, and water inlet velocities were 0.05 and 0.07 ms^{-1}. Water inlet temperatures were in range from 28 to 70°C.

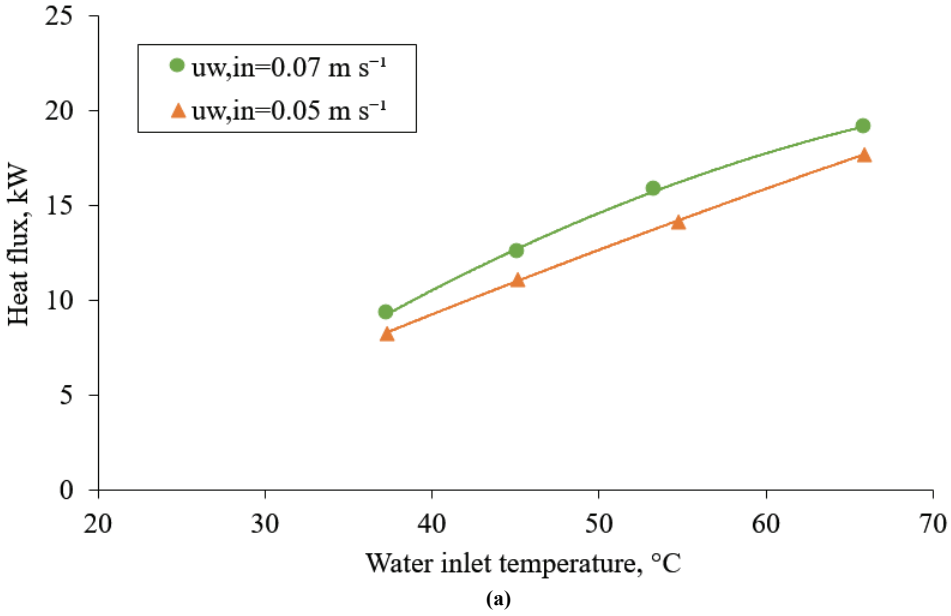

(a)

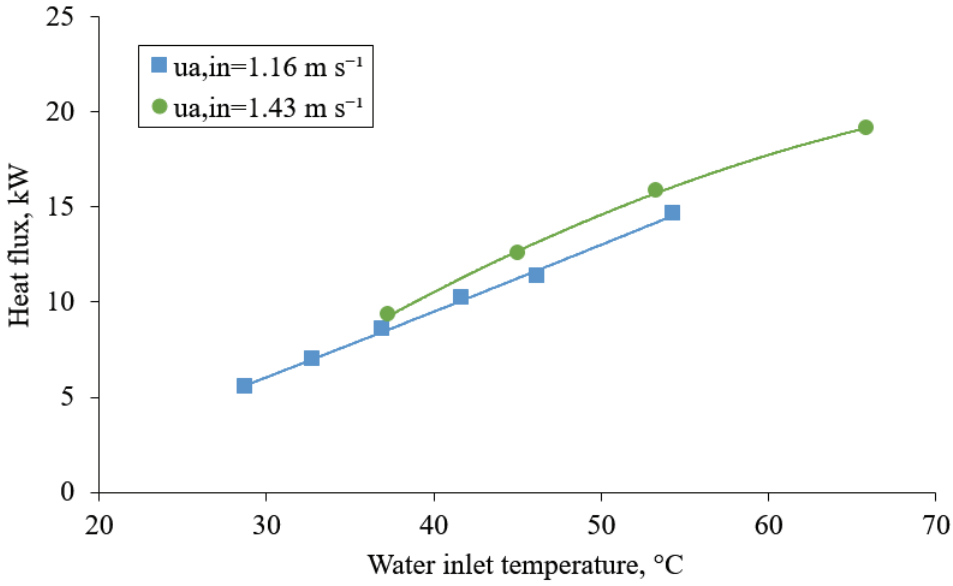

(b)

Fig. 12: Average exchanged heat fluxes for different water inlet temperatures in case of different water inlet velocities with test conditions: $T_{a,in}$ = 12°C, $u_{a,in}$ = 1.43 m s^{-1} (a) and different air inlet velocities with test conditions: $T_{a,in}$ = 12°C, $u_{w,in}$ = 0.07 m s^{-1} (b)

For whole range of water inlet temperatures, average heat flux is lower in cases of lower water inlet velocities and in cases of lower air inlet velocities.

Conclusion

Heat exchanger with microchannel coil has been installed in an open wind tunnel and measurements with different air and water flow and temperature regimes have been done. Measurements were performed in following range of air and water velocities and temperatures: air inlet velocities were from 0.5 to 5 m s^{-1}, water inlet velocities were in a range from 0.05 to 1 m s^{-1}, air and water inlet temperatures were in range from 2 to 68°C. Various parameter setups have been set and measurements were performed. Appropriate dependences of temperatures and exchanged heat fluxes on water and air inlet velocities have been shown. This paper presents a part of measurement results performed using modified and upgraded open circuit wind tunnel, with installed heat exchanger with microchannel coil. Main aim of this paper was to experimentally analyse the heat exchanger with microchannel coil in an air-water heat exchange application.

Goals of further work will be to improve heat balance in system and to make analysis of heat transfer efficiency. Acquired data from these measurements will be applied for validation of numerical model that will be used for optimization of heat exchanger with microchannel coil geometrical parameters.

*__Acknowledgement:__ This work has been fully supported by Croatian Science Foundation under the project HEXENER (IP-2016-06-4095).

References

Al-Zaidi, A.H., Mahmoud, M.M., Karayiannis, T.G., 2018. Condensation flow patterns and heat transfer in horizontal microchannels. Exp. Therm. Fluid. Sci. 90, 153-173, https://doi.org/10.1016/j.expthermflusci.2017.09.009

Asadi, M., Xie, G., Sunden, B., 2014. A review of heat transfer and pressure drop characteristics of single and two-phase microchannels, Heat Mass Transfer. 79, 34-53, https://doi.org/10.1016/j.ijheatmasstransfer.2014.07.090

Bhuiyan, A.A., Sadrul Islam, A.K.M., 2016. Thermal and hydraulic performance of finned-tube heat exchangers under different flow ranges: A review on modeling and experiment, Heat Mass Transfer. 101, 38-59, https://doi.org/10.1016/j.ijheatmasstransfer.2016.05.022

Bosnjakovic, F., 2012. Nauka o toplini, Graphis d.o.o., Zagreb (on Croatian).

Dalkilic, A.S., Mahian, O., Yilimaz, S., Sakamatapan, K., Wongwises, S., 2017. Experimental investigation of single-phase turbulent flow of R-134a in a multiport microchannel heat sink. Heat Mass Transfer. 89, 47-56, https://doi.org/10.1016/j.icheatmasstransfer.2017.09.023

Dalkilic, A.S., Özman, C., Sakamatapan, K., Wongwises, S., 2018. Experimental investigation on the flow boiling of R134a in a multi-microchannel heat sink. Heat. Mass. Transfer. 91, 125-137, DOI: 10.1016/j.icheatmasstransfer.2017.12.008

Danfoss, http://files.danfoss.com/technicalinfo/dila/24/DKQBPB400A402_Sep2014_LR.pdf, accessed on 6th of July, 2018.

Garcia, A., Wong, J., Diaz, G., Balkoski, K., Rico, K., 2011. Solar water heater utilizing mini-channel technology, The 2011 UC Solar Research Symposium, http://cast.ucmerced.edu/home/2011-solar-symposium, accessed on 6th of July, 2018.

Glazar, V., 2011. Compact Heat Exchanger Geometry Optimization. PhD thesis. Faculty of Engineering University of Rijeka, Croatia (in Croatian).

Glazar V., Frankovic B., Trp A., 2015. Experimental and numerical study of the compact heat exchanger with different microchannel shapes. Int. J. Refrig. 51 (1), 144-153, https://doi.org/10.1016/j.ijrefrig.2014.06.017

Kaltra Innovativtechnik, https://www.kaltra.de/microchannel-evaporators, accessed on 6th of July, 2018.

Kandlikar, S., Garimella, S., Li, D., Colin, S., King, M.R., 2016. Heat Transfer and Fluid Flow in Minichannels and Microchannels. Butterworth-Heinmann, United States of America.

Knourek, J., Kus, M., Syka, T., 2012. Measuring thermal characteristics of the heat exchanger. EPJ Web of Conferences 25, 01041, DOI: 10.1051/epjconf/20122501041.

Morini. G.L., 2004. Single-phase convective heat transfer in microchannels: a review of experimental results, Int. J. Therm. Sci. 43, 631-651, https://doi.org/10.1016/j.ijthermalsci.2004.01.003

Morini. G.L., 2006. Scaling Effects for Liquid Flows in Microchannels, Heat. Transfer Eng. 27, 64-73, https://doi.org/10.1080/01457630500523865Robles, A., Duong, V., Martin, A.J., Guadarrama, J.L., Diaz, G., 2014. Aluminum minichannel solar water heater performance under year-round weather conditions. Sol. Energy. 110, 356-364, https://doi.org/10.1016/j.solener.2014.09.031

Rosa, P., Karayiannis, T.G., Collins, M.W., 2009. Single-phase heat transfer in microchannels: The importance of scaling effects, Appl. Therm. Eng. 29, 3447-3468, https://doi.org/10.1016/j.applthermaleng.2009.05.015